

# Magnetic and Electronic Properties of $\text{Li}_x\text{CoO}_2$ Single Crystals

K. Miyoshi,<sup>1</sup> C. Iwai,<sup>1</sup> H. Kondo,<sup>1</sup> M. Miura,<sup>1</sup> S. Nishigori,<sup>2</sup> and J. Takeuchi<sup>1</sup>

<sup>1</sup>*Department of Material Science, Shimane University, Matsue 690-8504, Japan and*

<sup>2</sup>*Department of Materials Analysis, CIRS, Shimane University, Matsue 690-8504, Japan*  
(Dated: February 14, 2022)

Measurements of electrical resistivity ( $\rho$ ), DC magnetization ( $M$ ) and specific heat ( $C$ ) have been performed on layered oxide  $\text{Li}_x\text{CoO}_2$  ( $0.25 \leq x \leq 0.99$ ) using single crystal specimens. The  $\rho$  versus temperature ( $T$ ) curve for  $x=0.90$  and  $0.99$  is found to be insulating but a metallic behavior is observed for  $0.25 \leq x \leq 0.71$ . At  $T_S \sim 155$  K, a sharp anomaly is observed in the  $\rho$ - $T$ ,  $M$ - $T$  and  $C/T$ - $T$  curves for  $x=0.66$  with thermal hysteresis, indicating the first-order character of the transition. The transition at  $T_S \sim 155$  K is observed for the wide range of  $x=0.46$ – $0.71$ . It is found that the  $M$ - $T$  curve measured after rapid cool becomes different from that after slow cool below  $T_F$ , which is  $\sim 130$  K for  $x=0.46$ – $0.71$ .  $T_F$  is found to agree with the temperature at which the motional narrowing in the  $^7\text{Li}$  NMR line width is observed, indicating that the Li ions stop diffusing and order at the regular site below  $T_F$ . The ordering of Li ions below  $T_F \sim 130$  K is likely to be triggered and stabilized by the charge ordering in  $\text{CoO}_2$  layers below  $T_S$ .

PACS numbers: 75.40.Cx, 71.27.+a, 75.30.Kz

## I. INTRODUCTION

Layered oxide  $\text{Li}_x\text{CoO}_2$  has been intensively studied for the practical use as a high energy density cathode material in commercial Li ion batteries.  $\text{Li}_x\text{CoO}_2$  consists of  $\text{CoO}_2$  layers and interlayers of Li atoms alternatively stacked along  $c$  axis. The related material  $\text{Na}_x\text{CoO}_2$ , which is originally known as a large thermoelectric material,<sup>1</sup> has been a subject of intensive study since the discovery of superconductivity in  $\text{Na}_x\text{CoO}_2 \cdot 1.3\text{H}_2\text{O}$  below  $T_c \sim 5$  K.<sup>2</sup> In  $\text{CoO}_2$  layers, Co ions are in a mixed valence state nominally having spins of  $S=0$  ( $\text{Co}^{3+}$ ) and  $S=1/2$  ( $\text{Co}^{4+}$ ), and form a two-dimensional (2D) regular triangular lattice, where novel types of electronic behavior are expected due to the geometrical frustration. Indeed,  $\text{Na}_x\text{CoO}_2$  exhibits a rich variety of intriguing electronic properties as Na content  $x$  increases, that is, superconductivity in the hydrated compound ( $x \sim 0.35$ ),<sup>2</sup> an insulating ground state induced by charge ordering ( $x=0.5$ ),<sup>3–6</sup> unusual large thermoelectric power with metallic conductivity ( $x \sim 0.7$ ),<sup>1</sup> a mass-enhanced Fermi liquid ground state analogous to  $\text{LiV}_2\text{O}_4$  ( $x \sim 0.75$ ),<sup>7</sup> and a spin-density-wave state ( $x \geq 0.75$ ).<sup>8</sup>

$\text{Li}_x\text{CoO}_2$  has a similar structure with different stacking sequence of oxygen atom layers, where Li ions occupy the octahedral sites with three  $\text{CoO}_2$  sheets per unit cell, while Na ions in  $\text{Na}_x\text{CoO}_2$  occupy the prismatic sites with two  $\text{CoO}_2$  sheets per unit cell. Li deintercalation from  $\text{LiCoO}_2$  generates  $\text{Co}^{4+}$  ( $t_{2g}^5$ ) ions in the 2D triangular lattice of  $\text{Co}^{3+}$  ( $t_{2g}^6$ ) and leads to a hole doping in the  $t_{2g}$  orbitals. Although  $\text{LiCoO}_2$  is known to be insulating, a metallic behavior is therefore expected for the delithiated compound  $\text{Li}_x\text{CoO}_2$ . It has been reported that electrical resistivity near room temperature decreases abruptly with decreasing  $x$  from 1 to  $\sim 0.9$ ,<sup>9,10</sup> indicating a transition from insulator to metal.

For  $\text{Li}_x\text{CoO}_2$ , a sharp decrease in dc magnetization<sup>10–15</sup> and increase in resistivity<sup>7</sup> have been observed below 160–170 K with wide range of Li content. This transition is of first-order<sup>14,15</sup> and the occurrence of charge ordering in  $\text{CoO}_2$  layers has been suggested.<sup>12,15</sup> The fully delithiated compound  $\text{CoO}_2$  ( $x=0$ ), which is also the end member of  $\text{Na}_x\text{CoO}_2$ , has been found to be a Pauli paramagnetic metal without electron correlation due to the lack of two dimensionality in the structure contrasting to  $\text{A}_x\text{CoO}_2$  ( $\text{A}=\text{Li}, \text{Na}$ ).<sup>16</sup> Some attempts to establish the electronic phase diagram of  $\text{Li}_x\text{CoO}_2$  have been made through the synthesis for the full or nearly full range of  $x$  using an electrochemical reaction technique.<sup>12,15</sup> It is suggested that the critical Li content  $x_c$  at which the magnetic property changes from Pauli paramagnetic type to Curie-Weiss one is  $0.35$ – $0.45$ ,<sup>15</sup> whereas  $x_c$  for  $\text{Na}_x\text{CoO}_2$  is known to be  $0.5$ .<sup>3</sup>

In  $\text{Li}_x\text{CoO}_2$ , various unconventional nature may be discovered as in  $\text{Na}_x\text{CoO}_2$  due to the characteristic triangular  $\text{CoO}_2$  layers included in common in  $\text{A}_x\text{CoO}_2$ . Thus, it is interesting to explore the electronic behaviors of  $\text{Li}_x\text{CoO}_2$ , and it also allows to throw further light on the origin of the intriguing properties of  $\text{Na}_x\text{CoO}_2$ . Despite the recent intensive studies, details of the intrinsic properties of  $\text{Li}_x\text{CoO}_2$  still remain unclear. The investigations on  $\text{Li}_x\text{CoO}_2$  have been so far limited to the powder samples. For the further understanding, detailed investigations on the microscopic nature using single-crystal specimens are highly desirable in the future study. For the purpose, it is an important first step to synthesize single-crystal specimens of  $\text{Li}_x\text{CoO}_2$  with systematic change of  $x$  and survey the physical properties. In the present work, we have successfully synthesized single crystals of  $\text{Li}_x\text{CoO}_2$  with  $x=0.25$ – $0.99$  and performed the measurements of dc magnetization, electrical resistivity and specific heat. A first-order transition has been observed

at  $T_S \sim 155$  K for the specimen with  $x=0.46-0.71$ . We demonstrate that the transition at  $T_S$  is always followed by the ordering of Li ions below  $T_F \sim 130$  K. This suggests the possibility that the ordering of Li ions is triggered and stabilized by the charge ordering in  $\text{CoO}_2$  layers below  $T_S$  via Coulomb coupling.

## II. EXPERIMENT

Single crystal specimens of  $\text{Li}_x\text{CoO}_2$  were prepared by chemically extracting lithium from  $\text{LiCoO}_2$  single crystals reacting with an oxidizer  $\text{NO}_2\text{BF}_4$  in an acetonitrile medium. In the previous work, single crystals of  $\text{LiCoO}_2$  were grown in an optical floating-zone furnace,<sup>14</sup> whereas in the present work those were obtained by an ion exchange reaction between  $\text{Li}_2\text{CO}_3$  and  $\text{Na}_{0.75}\text{CoO}_2$  single crystals, which are easier to obtain than  $\text{LiCoO}_2$  single crystals. The single-crystal growth of  $\text{Na}_{0.75}\text{CoO}_2$  was performed in a similar manner as described in the literature.<sup>17</sup> Single crystals of  $\text{Na}_{0.75}\text{CoO}_2$  cleaved to a thickness of  $\sim 0.2$  mm were embedded in  $\text{Li}_2\text{CO}_3$  powder in an alumina boat and heated in air at  $600^\circ\text{C}$  for 24 h to exchange Na and Li ions. An ion exchange reaction with  $\text{LiNO}_3$  ( $250^\circ\text{C}$ , 48 h) is also useful to obtain  $\text{LiCoO}_2$  single crystals. After the reaction, the crystals were washed with distilled water repeatedly to remove  $\text{Li}_2\text{CO}_3$  and  $\text{Na}_2\text{CO}_3$ . Chemical extraction of lithium from  $\text{LiCoO}_2$  single crystals was carried out by immersing the crystals in an acetonitrile solution of  $\text{NO}_2\text{BF}_4$  under argon atmosphere at  $25-35^\circ\text{C}$  for 3 days. Molar ratio between  $\text{LiCoO}_2$  and  $\text{NO}_2\text{BF}_4$  was changed to control the Li content  $x$  ranging up to 1:2. The final products were washed with acetonitrile to remove  $\text{LiBF}_4$ . Synthesis of powder samples of  $\text{Li}_x\text{CoO}_2$  by delithiation using  $\text{NO}_2\text{BF}_4$  has been reported in the literature.<sup>18</sup> The Li content in the pristine and delithiated specimens was determined by inductively coupled plasma-atomic emission spectroscopy (ICP-AES). In this study, we used  $\text{Li}_x\text{CoO}_2$  single-crystal specimens with  $x=0.99$  (pristine), 0.90, 0.71, 0.66, 0.46 and 0.25. To confirm the phase purity of the specimens, powder X-ray diffraction (XRD) was performed by a conventional diffractometer (RINT2200, Rigaku) using  $\text{Cu K}\alpha$  radiation. Electrical resistivity was measured using a standard dc four-probe technique. dc magnetization measurements were carried out using superconducting quantum interference device magnetometer (MPMS, Quantum Design). Specific heat was measured by a thermal relaxation method on the physical property measurement system (PPMS, Quantum Design).

## III. RESULTS AND DISCUSSION

### A. Powder X-ray diffraction

In Fig. 1, powder XRD patterns for  $\text{Li}_x\text{CoO}_2$  with  $x=0.25-0.99$  are shown. Almost all of the peaks observed

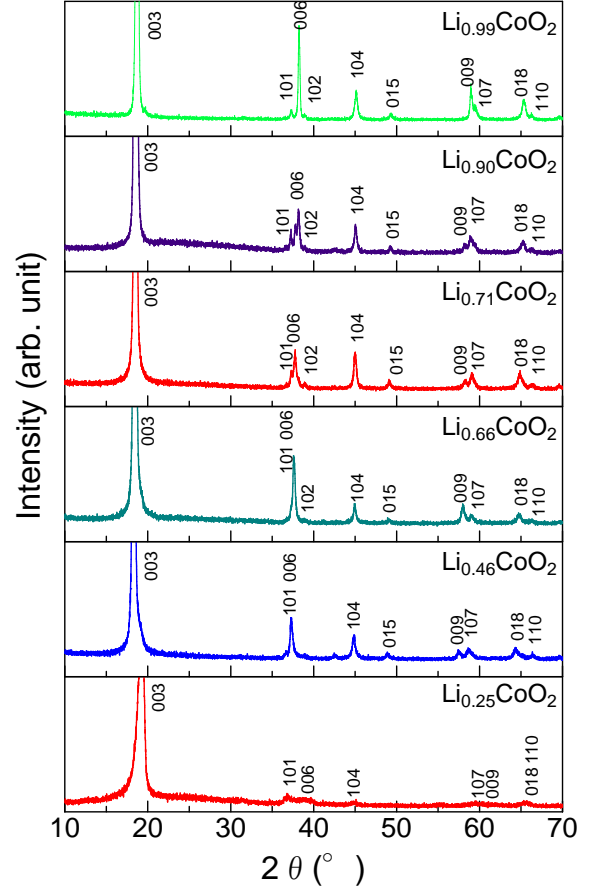


FIG. 1: (Color online) Powder X-ray diffraction patterns for  $\text{Li}_x\text{CoO}_2$  with  $x=0.25-0.99$ .

in XRD are indexed based on rhombohedral type space group  $R\bar{3}m$ , indicating that the samples are of single phase, although a splitting of the peak into two is readily observed in (003), (006) and (009) reflections for the specimen with  $x=0.90$ . The peak split is due to the existence of two hexagonal phase region for  $0.75 \leq x \leq 0.93$ , which has been widely observed in the electrochemical oxidation process by earlier workers.<sup>9,15,19-21</sup> Figure 2 displays plots of lattice parameter  $c$  versus  $x$  together with the variation in  $c$  during the electrochemical Li deintercalation observed by in-situ X-ray diffraction reproduced from Ref. 21. As seen in the figure, the variation of lattice parameter  $c$  of our specimens is consistent with that determined in the previous study. As the oxidation of  $\text{Li}_x\text{CoO}_2$  proceeds, a monoclinic phase appears in the neighborhood of  $x=0.5$  after the transition from hexagonal I to II for  $0.75 \leq x \leq 0.93$ , and hexagonal and monoclinic phases coexist for  $x \lesssim 0.20$ .<sup>19-21</sup> We note that more detailed structural phase diagram including the region for  $x < 0.2$  has been recently proposed through the measurements of quasi-open-circuit-voltage of  $\text{Li}_x\text{CoO}_2/\text{Al}$  cell.<sup>15</sup>

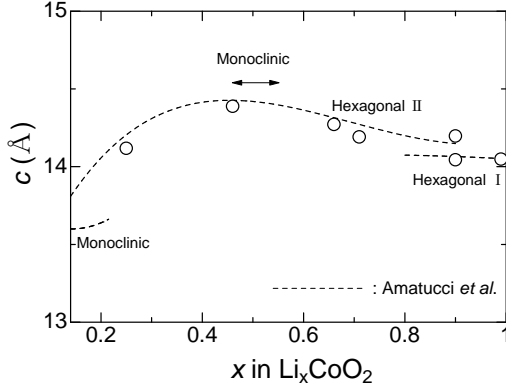


FIG. 2: Lattice parameter  $c$  for  $\text{Li}_x\text{CoO}_2$  with  $x=0.25-0.99$ . The dotted lines show the variation of  $c$  for  $\text{Li}_x\text{CoO}_2$  observed by in-situ X-ray diffraction during the electrochemical Li deintercalation by Amatucci *et al* (Ref. 21). Hexagonal and monoclinic phases appear in the oxidation process.

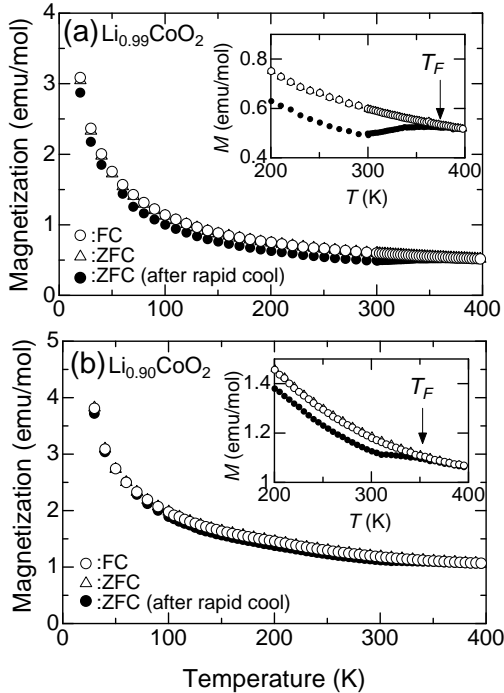


FIG. 3: Temperature dependence of dc magnetization measured with a magnetic field of  $H=1$  T parallel to  $ab$ -plane for  $\text{Li}_x\text{CoO}_2$  with  $x=0.99$  (a) and  $0.90$  (b). The measurements were done after rapid cool from above 400 K to 10 K (closed circles) in addition to the measurements after slow cool down to 10 K (open symbols). The insets show close ups of the data for  $200 \leq T \leq 400$  K.

### B. dc magnetization

In Figs. 3(a) and 3(b), we show the results of the dc magnetization ( $M$ ) measurements as a function of temperature ( $T$ ) for  $\text{Li}_x\text{CoO}_2$  with  $x=0.99$  and  $0.90$  mea-

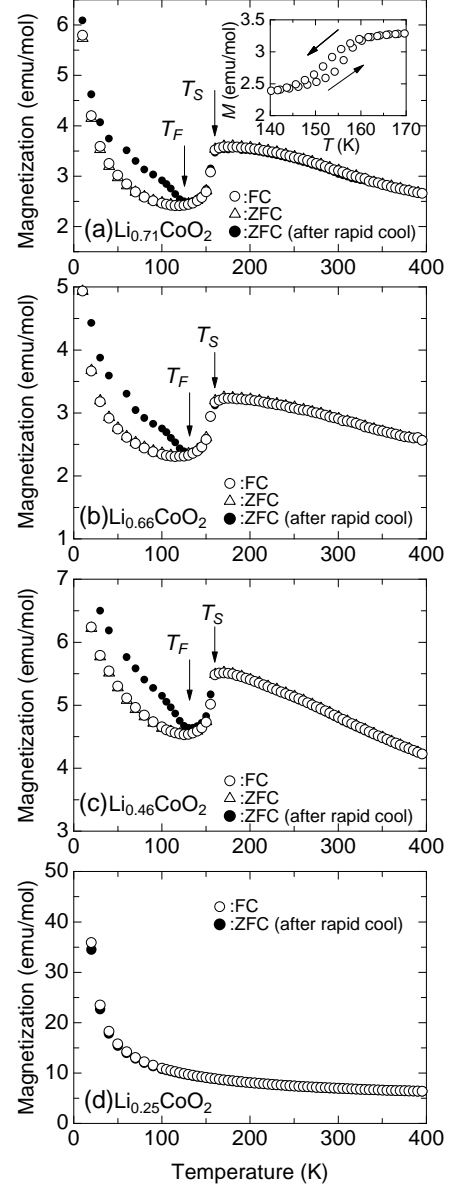


FIG. 4: Temperature dependence of dc magnetization measured with a magnetic field of  $H=1$  T parallel to  $ab$ -plane for  $\text{Li}_x\text{CoO}_2$  with  $x=0.71$  (a),  $0.66$  (b),  $0.46$  (c) and  $0.25$  (d). The measurements were done after rapid cool from 400 K to 10 K (closed circles) in addition to the measurements after slow cool down to 10 K (open symbols). The inset shows the data collected during heating and cooling between 140 K and 170 K for  $x=0.66$ .

sured with an applied magnetic field of  $H=1$  T parallel to  $ab$ -plane under zero-field-cooled (ZFC) and field-cooled (FC) condition. In the measurements, dc magnetization was first measured up to 400 K after rapid cool of the sample from above 400 K to 10 K in zero field. For rapid cool, the sample was once heated above 400 K in an electric furnace and quenched in acetonitrile at room temperature. This was followed by rapid sample

insertion into the chamber of the magnetometer kept at 10 K. Then, the measurements were performed again after slow cool from 400 K to 10 K at a rate  $-10$  K/min. in zero field and in a magnetic field of 1 T. As seen in Figs. 3(a) and 3(b), the  $M(T)$  curve after slow cool both for  $x=0.99$  and  $0.90$  appears to show a Curie-Weiss type paramagnetic behavior and any difference is not observed in the FC and ZFC measurements, indicating the absence of magnetic order. On the other hand, the  $M(T)$  curve after rapid cool for  $x=0.99$  becomes different from those after slow cool below  $T_F \sim 380$  K, as seen in the inset of Fig. 3(a). Also, it is found in the inset of Fig. 3(b) that the  $M(T)$  curve for  $x=0.90$  becomes thermal history dependent below  $T_F \sim 350$  K.

In Figs. 4(a)-4(d), the  $M(T)$  curves for  $\text{Li}_x\text{CoO}_2$  with  $x=0.25-0.71$  are shown. The measurements for  $x=0.25-0.71$  were also performed both after rapid and slow cool in a similar manner to those for  $x=0.90$  and  $0.99$ . In Fig. 4(a), the  $M(T)$  curves for  $x=0.71$  exhibit a sharp decrease below  $T_S \sim 155$  K. As shown in the inset of Fig. 3(a), a thermal hysteresis is observed in the  $M(T)$  curve for  $x=0.71$  around  $T_S$ , indicating the transition at  $T_S$  is of first-order. These behaviors have been similarly observed in earlier studies.<sup>10-15</sup> Also it is found that there is no difference in the  $M_{\text{FC}}(T)$  and  $M_{\text{ZFC}}(T)$  curves after slow cool, but the  $M(T)$  curves after slow and rapid cool exhibit a splitting below  $T_F \sim 130$  K. The characteristic behaviors of the  $M(T)$  curve for  $x=0.71$  are similarly observed for  $x=0.66$  and  $0.46$  as seen in Figs. 4(b) and 4(c). It is noted that  $T_S$  ( $\sim 155$  K) and  $T_F$  ( $\sim 130$  K) appears to be independent of Li content  $x$  for  $0.46 \leq x \leq 0.71$ . As shown later,  $T_F$  agrees with the temperature at which the motional narrowing in the  $^7\text{Li}$  NMR line width is observed, indicating that the Li ions stop diffusing and stay at the regular site below  $T_F$ .

In Fig. 4(d), the  $M(T)$  curve for  $x=0.25$  is found to exhibit no anomaly contrasting to the sample with  $0.46 \leq x \leq 0.71$  but a Curie-Weiss-like  $T$ -dependence with no sign of magnetic order.  $\chi(T)$  [ $=M(T)/H$ ] curve for  $x=0.99$ ,  $0.90$  and  $0.25$  observed in the FC measurements was fitted with the following formula:

$$\chi(T) = \chi_0 + \frac{C}{T - \Theta}, \quad (1)$$

where  $\chi_0$ ,  $C$  and  $\Theta$  denote the  $T$ -independent susceptibility, the Curie constant and the Weiss temperature, respectively. Fitting parameters obtained from the fits of the  $\chi(T)$  data ( $10 \leq T \leq 400$  K) to Eq. (1) are summarized in Table 1. In the Table, effective magnetic moment  $\mu_{\text{eff}}$  per Co atom was calculated from  $C$ , considering that all of the Co atoms are equivalent, while  $\mu_{\text{eff}}$  per  $\text{Co}^{4+}$  was calculated assuming that all of the  $\text{Co}^{3+}$  ions are nonmagnetic ( $S=0$ ). Although  $\mu_{\text{eff}}$  per  $\text{Co}^{4+}$  is  $\sim 2.7 \mu_B$  for  $x=0.99$ ,  $\mu_{\text{eff}}$  yields  $1.73 \mu_B$  corresponding to low spin  $\text{Co}^{4+}$  ( $S=1/2$ ) if we assume  $x \sim 0.975$ . An error range  $\Delta x = \pm 0.015$  of the composition determined by ICP may be possible for  $x=0.99$ . The value of  $\mu_{\text{eff}}$  per  $\text{Co}^{4+}$  is reduced to  $\sim 1.1 \mu_B$  for the sample with  $x=0.90$ ,

which is near the boundary between metallic and insulating states, as seen later. For  $x=0.25$ ,  $\mu_{\text{eff}}$  per  $\text{Co}^{4+}$  still has a large value of  $\sim 0.83 \mu_B$ , whereas it has been reported that  $\text{Li}_x\text{CoO}_2$  obtained by electrochemical oxidation is Pauli paramagnetic for  $x \lesssim 0.35$ .<sup>15</sup> In the table, it is found that  $\Theta$  has a small negative value and  $\chi_0$  becomes larger with decreasing  $x$  probably due to the increase of Pauli paramagnetic component. These features are also found in the electrochemically delithiated specimens.<sup>15</sup>

### C. Electrical resistivity

Next, we show the temperature dependence of electrical resistivity ( $\rho$ ) for  $\text{Li}_x\text{CoO}_2$  with  $x=0.25-0.99$  in Figs. 5(a)-5(e). The data shown in the figures were collected during heating after slow cool down to  $\sim 10$  K ( $\sim -2$  K/min.). For  $x=0.99$ , the  $\rho(T)$  curve exhibits an insulating behavior in Fig. 5(a). The  $\rho(T)$  curve for  $x=0.99$  was confirmed not to strictly obey an Arrhenius law, having a slightly temperature depending activation energy of  $E_a \sim 0.03$  eV for  $T=100-300$  K and  $\sim 0.02$  eV for  $T < 100$  K. Also, an insulating behavior of  $\rho(T)$  with an activation energy of  $10^{-2}$  eV order which varies slightly with temperature has been observed in  $\text{Li}_x\text{CoO}_2$  with  $x=0.98-0.96$  in an earlier study.<sup>9</sup> For  $x=0.90$ , the  $\rho(T)$  curve is nearly temperature independent with resistivity  $\sim 10^0 \Omega\text{cm}$ , which is  $\sim 50$  times smaller than that for  $x=0.99$  at 300 K. In Fig. 5(b), the  $\rho(T)$  curve for  $x=0.71$  displays a metallic behavior with an amplitude of  $\text{m}\Omega\text{cm}$  order. Thus, the critical Li content at which the system changes from an insulator to metal is likely to be near below 0.90. The  $\rho(T)$  curve for  $x=0.71$  shows a sudden increase below  $\sim 155$  K, which corresponds to the first-order transition observed in the  $M(T)$  curve at  $T_S \sim 155$  K. Although a formation of charge ordered state in  $\text{CoO}_2$  layers has been expected for  $x=2/3$ ,<sup>15</sup> no indicative of a transition into an insulating state is found in the  $\rho(T)$  curve. However, we should note that the slope of the  $\rho(T)$  curve for  $x=0.71$  becomes smaller below the jump at  $T_S \sim 155$  K, suggesting that the transport mechanism changes below  $T_S$ . The  $\rho(T)$  curve for  $x=0.66$  is qualitatively similar to that for  $x=0.71$ , as seen in Fig. 5(c). For  $x=0.66$ , the data collected during cooling are also shown. A slight thermal hysteresis is found in the jump-like anomaly at  $T_S$  as a result of the first-order character of the transition. The  $\rho(T)$  curve for  $x=0.46$  in Fig. 5(d) also shows an anomaly at  $T_S \sim 155$  K but the anomaly is relatively small. In contrast, there is no anomaly in the  $\rho(T)$  curve for  $x=0.25$  in Fig. 5(e). Moreover, the residual resistivity of the  $\rho(T)$  curve for  $x=0.25$  is relatively small compared with that for higher  $x$ . The higher metallicity for  $x=0.25$  may be associated with the absence of the transition at  $T_S$ .

TABLE I: Constant susceptibility  $\chi_0$ , Weiss temperature  $\Theta$ , Curie constant  $C$ , and effective magnetic moment  $\mu_{\text{eff}}$  for  $\text{Li}_x\text{CoO}_2$  with  $x=0.99, 0.90$  and  $0.25$ . These parameters were extracted from the  $M(T)$  data ( $10 \leq T \leq 400$  K) using Eq. (1).

$x$	$\chi_0$ (emu/mol/Oe)	$\Theta$ (K)	$C$ (emu/mol/K/Oe)	$\mu_{\text{eff}}$ ( $\mu_B/\text{Co}$ )	$\mu_{\text{eff}}$ ( $\mu_B/\text{Co}^{4+}$ )
0.99	$2.95 \times 10^{-5}$	-11	$9.31 \times 10^{-3}$	0.273	2.73
0.90	$7.33 \times 10^{-5}$	-9.4	$1.40 \times 10^{-2}$	0.335	1.06
0.25	$4.81 \times 10^{-4}$	-3.2	$6.48 \times 10^{-2}$	0.720	0.831

#### D. Specific heat

Figure 6 displays plots of specific heat divided by temperature  $C/T$  versus  $T$  for  $\text{Li}_{0.66}\text{CoO}_2$ . The measurements were performed during cooling and heating after slow cool ( $-10$  K/min.). The data measured during heating show a sharp peak corresponding to the transition at  $T_S \sim 155$  K, while those measured on cooling show a small peak. A large thermal hysteresis is observed as a strong

evidence of the first-order character of the transition at  $T_S$ . The measurements were also carried out in a magnetic field of  $H=9$  T. The  $C/T$  peak at  $T_S$  is found to be not field dependent, indicating that the transition is not magnetic one. Assuming the occurrence of charge ordering at the fractional Li content  $x=2/3$ , the transition entropy is calculated as  $\Delta S = -R(1/3 \ln 1/3 + 2/3 \ln 2/3) = 5.29$  J/mol K, which is the mixing entropy of  $\text{Co}^{3+}/\text{Co}^{4+}$  solution. To examine whether or not the transition entropy at  $T_S$  for  $x=0.66$  corresponds to that of the charge ordering for  $x=2/3$ , we have estimated the entropy  $S$  as a function of  $T$  from the electronic contribution of specific heat  $C_e$  using the thermodynamic relationship,

$$S(T) = \int_0^T \frac{C_e}{T'} dT'. \quad (2)$$

$C_e$  is given by subtracting the lattice contribution  $C_{\text{lat}}$  from the measured specific heat  $C$ . The  $C_{\text{lat}}(T)$  data were estimated from the  $C(T)$  data for insulating  $\text{Li}_{0.99}\text{CoO}_2$ . In the inset of Fig. 6, the  $S(T)$  curve obtained by integrating  $C_e/T$  above 2 K is shown. The transition entropy is estimated to be  $\Delta S \sim 1.9$  J/molK for  $T=140-170$  K. This value is 36% of the transition entropy of charge ordering for  $x=2/3$ , suggesting the possibility that the charge ordering is incomplete and a part of carriers are localized. This scenario agrees with the result that  $\rho(T)$  curve for  $x=0.66$  exhibits a sudden increase at  $T_S$  but is still metallic below  $T_S$ . The transition entropy for  $\text{Li}_x\text{CoO}_2$  with  $x=0.67$  has been found to be  $\Delta S = 1.49$  J/molK from the magnitude of latent heat in the differential scanning calorimetry (DSC) measurements.<sup>15</sup> In a similar context, it has been argued from the smaller  $\Delta S$  that the charge ordering is incomplete and a charge disproportionation e.g.,  $2\text{Co}^{+3.5} \rightarrow \text{Co}^{+3.5+\delta} + \text{Co}^{+3.5-\delta}$  occurs.<sup>15</sup> Also for  $x=0.71$ , a sharp anomaly at  $T_S$  was observed in  $C(T)/T$  data. For  $x=0.46$ , no distinct anomaly was however observed at  $T_S$ . This leads us to remember that the anomaly in the  $\rho(T)$  curve for  $x=0.46$  is relatively small compared to that for  $x=0.66$  and  $0.71$ . The DSC measurements have also revealed that the transition entropy for  $x=0.50$  is  $\Delta S = 0.47$  J/molK, which is considerably smaller than that for  $x=0.67$ .<sup>15</sup> Thus, it is inferred that the volume fraction of the charge ordering at  $T_S$  becomes continuously smaller with decreasing  $x$  and may be negligible for  $x < 0.40-0.45$ .

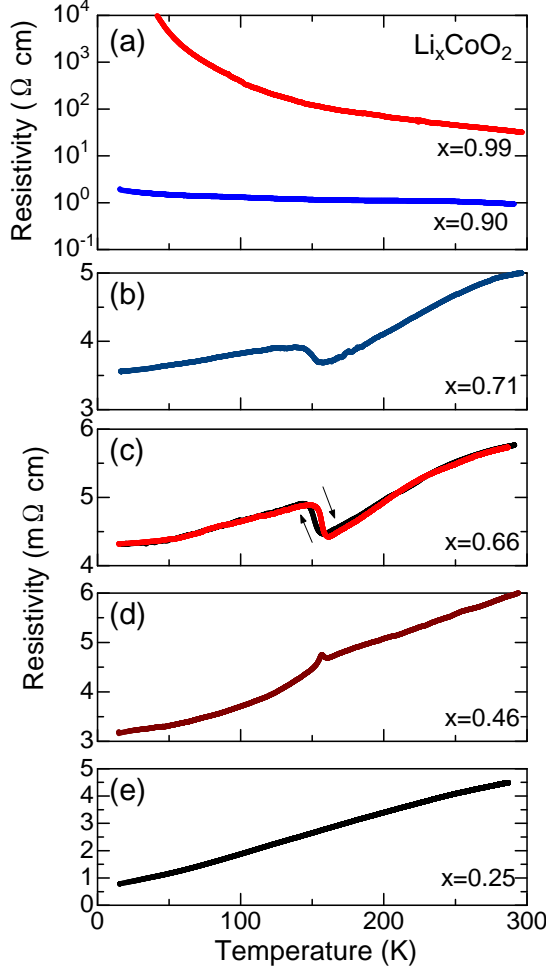


FIG. 5: (Color online) Temperature dependence of electrical resistivity measured along  $ab$ -plane for  $\text{Li}_x\text{CoO}_2$  with  $x=0.99, 0.90$  (a),  $0.71$  (b),  $0.66$  (c),  $0.46$  (d) and  $0.25$  (e).

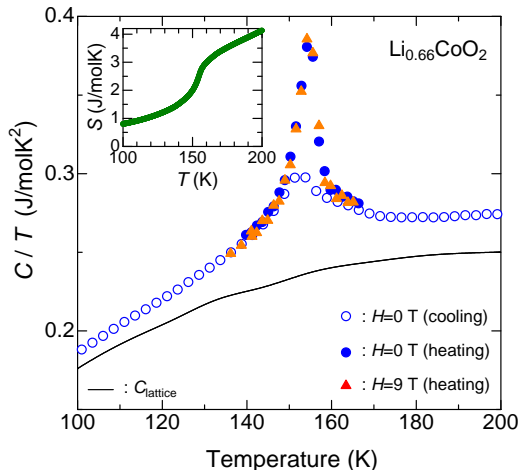


FIG. 6: (Color online) Plots of specific heat divided by temperature  $C/T$  versus temperature  $T$  for  $\text{Li}_{0.66}\text{CoO}_2$  at  $H=0$  and 9 T. The magnetic field was applied parallel to the  $c$ -axis. The data were collected during heating (closed symbols) and cooling (open circles). The solid line represents the lattice contribution. The inset shows magnetic entropy versus temperature curve.

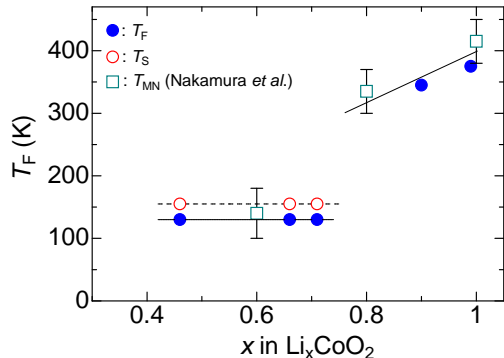


FIG. 7: (Color online) Plots of  $T_F$  versus  $x$  for  $\text{Li}_x\text{CoO}_2$ .  $T_S$  and  $T_{MN}$  are also plotted.  $T_{MN}$  is the temperature at which the motional narrowing in the  $^7\text{Li}$  NMR line width has been observed (Ref. 22). The solid and dotted lines are guides for the eyes.

### E. Plots of $T_F$ versus Li content $x$

In the dc magnetic measurements,  $T_F$ , below which the  $M(T)$  curve measured after rapid cool becomes different from that after slow cool, has been determined for each  $x$ . We show the plots of  $T_F$  versus  $x$  in Fig. 7, where  $T_S$  and the temperature at which the motional narrowing in the  $^7\text{Li}$  NMR line width has been observed ( $T_{MN}$ )<sup>22</sup> are plotted together. For higher  $x$  ( $\geq 0.90$ ),  $T_F$  decreases with decreasing  $x$ . In contrast,  $T_F$  is  $x$ -independent for  $x \lesssim 0.7$ . It is found that the characteristic relationship between  $T_F$  and  $x$  are in good agreement with  $T_{MN}$  versus  $x$  data, suggesting that  $T_F$  corresponds to the temperature above

which Li ions start to diffuse from the regular site. This is also supported by the recent  $\mu^+\text{SR}$  experiments on  $\text{Li}_x\text{CoO}_2$ , which have revealed that the Li diffusion starts above  $T_d^{\text{Li}} \sim 150$  K both for  $x=0.73$  and 0.53.<sup>23</sup> This fact is a firm evidence for the reliability of our result that the onset temperature of Li diffusion is  $x$ -independent for  $0.45 \lesssim x \lesssim 0.70$ . The slight difference between  $T_d^{\text{Li}}$  ( $\sim 150$  K) and  $T_F$  ( $\sim 130$  K) may be due to the difference of the sample. The sample used in the  $\mu^+\text{SR}$  experiments shows a sudden decrease of  $M(T)$  at  $\sim 170$  K, which is also slightly higher than  $T_S \sim 155$  K of our specimens. We have found in this study that the difference in the  $M(T)$  curve after slow and rapid cool is a reliable marker to detect the onset of Li diffusion.

### F. Discussion

In  $\text{Li}_x\text{CoO}_2$ , Li ions stop diffusing and the ordering of Li ions is stabilized below  $T_F$ . The origin of the  $\text{Li}^+$  ordering for  $x \lesssim 0.7$  and  $x \gtrsim 0.8$  is considered to be different from each other, since  $T_F$  suddenly decreases and becomes constant for  $x \lesssim 0.7$ . As seen in Fig. 7, the first order transition at  $T_S$  is always followed by the  $\text{Li}^+$  ordering below  $T_F \sim 130$  K, suggesting the possibility that the ordering of Li ions is triggered and stabilized by the charge ordering in  $\text{CoO}_2$  layers below  $T_S$ , where electrons combine with cobalt ions. This situation reminds us an intimate correlation between  $\text{Co}^{3+}/\text{Co}^{4+}$  charge ordering and  $\text{Na}^+$  ordering (zigzag chain) observed in  $\text{Na}_{0.5}\text{CoO}_2$ <sup>6</sup>, and also the characteristic ordering pattern of  $\text{Na}^+$  vacancies in  $\text{Na}_{0.75}\text{CoO}_2$  which provides an electrostatic landscape on the Co layers affecting the electronic and magnetic properties.<sup>24–26</sup> For  $x=0.66$ , we have observed a fairly small transition entropy at  $T_S$  compared with that expected in the transition into charge ordered state for  $x=2/3$ , in addition to a metallic behavior in the  $\rho(T)$  curve even below  $T_S$ . This suggests that the carrier localization below  $T_S$  is partial. Indeed, an electronic disproportionation at Co sites has been observed in  $\text{Na}_{0.75}\text{CoO}_2$ , where only 30% of the Co site form an ordered pattern of localized  $\text{Co}^{3+}$  states.<sup>27</sup> Moreover, we should note that this electronic texture in the  $\text{CoO}_2$  layers would contribute to stabilizing the ordering of Na ions,<sup>27</sup> as recent calculation also suggest.<sup>28</sup> Thus, the charge ordering coupled with the  $\text{Li}^+$  ordering in  $\text{Li}_x\text{CoO}_2$  may be analogous to that observed in  $\text{Na}_{0.75}\text{CoO}_2$ . The difference in the aspects of charge ordering between  $\text{Li}_x\text{CoO}_2$  and  $\text{Na}_x\text{CoO}_2$  is however obvious, since an insulating state is established by the complete charge ordering in  $\text{Na}_{0.5}\text{CoO}_2$ . To clarify the origin of the difference, the investigations on the ordering patterns of Li ions in  $\text{Li}_x\text{CoO}_2$  at low  $T$  and comparison with that in  $\text{Na}_x\text{CoO}_2$  are highly desirable.

Next, we focus on the behavior of  $M(T)$  curve, which depends on thermal history showing a different amplitude of  $M$  for the measurements after rapid and slow cool, as shown in Figs. 3 and 4. The ordering pat-

tern of Li ions after rapid cool is likely to be different from that after slow cool due to the glass-like freezing of the  $\text{Li}^+$  motions by rapid cooling, and should be linked with the ordering of  $\text{Co}^{3+}/\text{Co}^{4+}$  via Coulomb interactions, which determines the amplitude of  $M$ . Thus, rapid cooling introduces disorder in Li layers, which would disturb the charge ordering in Co layers expected for  $x=0.46\text{--}0.71$  below  $T_S$ . The destruction of the charge ordering may lead to the enhancement of  $M$  at low  $T$ , since the  $M(T)$  curve exhibits a sudden increase above  $T_S$  where the charge ordering is completely destroyed. In Figs. 4(a)–4(c), the amplitude of  $M(T)$  after rapid cool is indeed enhanced compared to that after slow cool at low  $T$  and they coincide above  $T_F$ , where Li ions can diffuse so that the charge ordering in Co layers is reproduced. However, we could not observe a clear anomaly in the  $\rho(T)$  curve at  $T_F$  for  $x=0.46\text{--}0.71$  even in the measurement after rapid cool, because the number of electrons which contributes to the metallic conductivity never changes across  $T_F$ . Forming a contrast,  $M(T)$  measured after rapid cool is smaller than that after slow cool for  $x=0.90$  and  $0.99$ , as seen in Fig 3. In this case, the arrangement of Li ions at high  $T$  also would be preserved by the freezing of  $\text{Li}^+$  motions after rapid cool, and the difference of  $M(T)$  below  $T_F$  should also originate from the difference in the arrangements of Li ions below  $T_F$ . We note that the hysteresis observed for  $x=0.99$  is rather larger than that for  $x=0.90$ . The larger hysteresis seems to be associated with the larger Li content in  $\text{Li}_{0.99}\text{CoO}_2$ , although the detailed mechanism is unclear. We could not rule out the possibility that Li layers are formed in an amorphous state by rapid cooling. If it is the case, the difference in the structure in Li layers could arise even for  $x\sim 1.0$  and is necessary to explain the large thermal history dependence in the  $M(T)$  curve for  $x=0.99$ .

#### IV. SUMMARY

In the present work, we have successfully obtained single crystals of  $\text{Li}_x\text{CoO}_2$  with  $x=0.25\text{--}0.99$  and per-

formed the measurements of DC magnetization, electrical resistivity and specific heat. It is found that the system changes from an insulator to metal at the critical Li content near below  $x=0.90$  with decreasing  $x$ . A first-order phase transition is observed at  $T_S\sim 155$  K for  $x=0.46\text{--}0.71$ .  $T_F$  below which the  $M(T)$  curve becomes thermal history dependent is found to correspond to the onset temperature of  $\text{Li}^+$  diffusion. For  $x=0.46\text{--}0.71$ , the first-order transition at  $T_S\sim 155$  K is always followed by the ordering of Li ions below  $T_F\sim 130$  K, suggesting the possibility that the ordering of Li ions is triggered and stabilized by the charge ordering in Co layers. The transition entropy for  $x=0.66$  estimated from the specific heat anomaly is found to be  $1.9$  mJ/molK, which is  $\sim 36\%$  of that for the complete  $\text{Co}^{3+}/\text{Co}^{4+}$  charge ordering in  $\text{Li}_{2/3}\text{CoO}_2$ . In addition, the  $\rho(T)$  curve for  $x=0.66$  exhibits a sudden increase but still metallic below  $T_S$ . These facts suggest that the carrier localization below  $T_S$  is in part. It is inferred that the volume fraction of the charge ordering below  $T_S$  becomes continuously smaller with decreasing  $x$  and may be negligible for  $x<0.40\text{--}0.45$ . For the further understanding, microscopic investigations on  $\text{Li}_x\text{CoO}_2$  ( $0.4\lesssim x\lesssim 0.7$ ) using single crystal specimens are urgently required. Also, it is important to establish the ordering patterns of Li ions at low  $T$ , since there would be a strong correlation between the ordering of  $\text{Li}^+$  and the charge ordering in Co layers due to the electrostatic landscape provided by  $\text{Li}^+$  ordering as in  $\text{Na}_x\text{CoO}_2$ .<sup>24,26</sup>

#### Acknowledgments

This work is financially supported by a Grant-in-Aid for Scientific Research (No. 20540355) from the Japanese Ministry of Education, Culture, Sports, Science and Technology.

<sup>1</sup> I. Terasaki, Y. Sasago, and K. Uchinokura, Phys. Rev. B **56**, R12685 (1997).

<sup>2</sup> K. Takeda, H. Sakurai, E. Takayama-Muromachi and F. Izumi, R. A. Dilanian, and T. Sasaki, Nature **422**, 53 (2003).

<sup>3</sup> M. L. Foo, Y. Wang, S. Watauchi, H. W. Zandbergen, T. He, R. J. Cava, and N. P. Ong, Phys. Rev. Lett. **92**, 247001 (2004).

<sup>4</sup> M. Yokoi, T. Moyoshi, Y. Kobayashi, M. Soda, Y. Yasui, M. Sato, and K. Kakurai, J. Phys. Soc. Japan **74**, 3046 (2005).

<sup>5</sup> G. Gašparović, R. A. Ott, J. -H. Cho, F. C. Chou, Y. Chu, J. W. Lynn and Y. S. Lee, Phys. Rev. Lett. **96**, 046403 (2006).

<sup>6</sup> F. L. Ning, S. M. Golin, K. Ahilan, T. Imai, G. J. Shu, and F. C. Chou, Phys. Rev. Lett. **100**, 086405 (2008).

<sup>7</sup> K. Miyoshi, E. Morikuni, K. Fujiwara, J. Takeuchi, and T. Hamasaki, Phys. Rev. B **69**, 132412 (2004).

<sup>8</sup> T. Motohashi, R. Ueda, E. Naujalis, T. Tojo, I. Terasaki, T. Atake, M. Karppinen, and H. Yamauchi, Phys. Rev. B **67**, 064406 (2003).

<sup>9</sup> M. Ménétrier, I. Saadoune, S. Levasseur, and C. Delmas, J. Mater. Chem. **9**, 1135 (1999).

<sup>10</sup> D. G. Kellerman, V. R. Galakhov, A. S. Semenov, Ya. N. Blinovskov, and O. N. Leonidova, Phys. Solid State **48**, 548 (2006).

<sup>11</sup> J. Sugiyama, H. Nozaki, J. H. Brewer, E. J. Ansaldo, G. D. Morris, and C. Delmas, Phys. Rev. B **72**, 144424 (2005).



- <sup>12</sup> K. Mukai, Y. Ikeda, H. Nozaki, J. Sugiyama, K. Nishiyama, D. Andreica, A. Amato, P. L. Russo, E. J. Ansaldo, J. H. Brewer, K. H. Chow, K. Ariyoshi, and T. Ohzuku, *Phys. Rev. Lett.* **99**, 087601 (2007).
- <sup>13</sup> J. T. Hertz, Q. Huang, T. McQueen, T. Klimczuk, J. W. G. Bos, L. Viciu, and R. J. Cava, *Phys. Rev. B* **77**, 075119 (2008).
- <sup>14</sup> K. Miyoshi, H. Kondo, M. Miura, C. Iwai, K. Fujiwara, and J. Takeuchi, *J. Phys. Conference Series* **150**, 042129 (2009).
- <sup>15</sup> T. Motohashi, T. Ono, Y. Sugimoto, Y. Masubuchi, S. Kikkawa, R. Kanno, M. Karppinen, and H. Yamauchi, *Phys. Rev. B* **80**, 165114 (2009).
- <sup>16</sup> S. Kawasaki, T. Motohashi, K. Shimada, T. Ono, R. Kanno, M. Karppinen, H. Yamauchi, and Guo-qing Zheng, *Phys. Rev. B* **79**, 220514(R) (2009).
- <sup>17</sup> F. C. Chou, J. H. Cho, P. A. Lee, E. T. Abel, K. Matan, and Y. S. Lee, *Phys. Rev. Lett.* **92**, 157004 (2004).
- <sup>18</sup> S. Venkatraman and A. Manthiram, *Chem. Mater.* **14**, 3907 (2002).
- <sup>19</sup> J. N. Reimers and J. R. Dahn, *J. Electrochem. Soc.* **139**, 2091 (1992).
- <sup>20</sup> T. Ohzuku and A. Ueda, *J. Electrochem. Soc.* **141**, 2972 (1994).
- <sup>21</sup> G. G. Amatucci, J. M. Tarascon, and L. C. Klein, *J. Electrochem. Soc.*, **143**, 1114 (1996).
- <sup>22</sup> K. Nakamura, H. Ohno, K. Okamura, Y. Michihiro, T. Moriga, I. Nakabayashi, and T. Kanashiro, *Solid State Ionics* **177**, 821 (2006).
- <sup>23</sup> J. Sugiyama, K. Mukai, Y. Ikeda, H. Nozaki, M. Mansson, and I. Watanabe, *Phys. Rev. Lett.* **103**, 147601 (2009).
- <sup>24</sup> M. Roger, D. J. P. Morris, D. A. Tennant, M. J. Gutmann, J. P. Goff, J.-U. Hoffmann, R. Feyerherm, E. Dudzik, D. Prabhakaran, A. T. Boothroyd, N. Shannon, B. Lake, and P. P. Deen, *Nature (London)* **445**, 631 (2007).
- <sup>25</sup> F. C. Chou, M. -W. Chu, G. J. Shu, F.-T. Huang, W. W. Pai, H. S. Sheu, and P. A. Lee, *Phys. Rev. Lett.* **101**, 127404 (2008).
- <sup>26</sup> D. J. P. Morris, M. Roger, M. J. Gutmann, J. P. Goff, D. A. Tennant, D. Prabhakaran, A. T. Boothroyd, E. Dudzik, R. Feyerherm, J.-U. Hoffmann, and K. Kiefer, *Phys. Rev. B* **79**, 100103(R) (2009).
- <sup>27</sup> M. -H. Julien, C. de Vaulx, H. Mayaffre, C. Berthier, M. Horvatić, V. Simonet, J. Wooldridge, G. Balakrishnan, M. R. Lees, D. P. Chen, C. T. Lin, and P. Lejay, *Phys. Rev. Lett.* **100**, 096405 (2008).
- <sup>28</sup> Y. S. Meng, A. Van der Ven, M. K. Y. Chan, and G. Ceder, *Phys. Rev. B* **72**, 172103 (2005).